J Solid State Electrochem (2011) 15:2639–2644
DOI 10.1007/s10008-010-1251-1

ORIGINAL PAPER

# Electrodeposition and characterization of assembly of Sn on Cu nanorods for Li-ion microbattery application

**Dongdong Jiang · Haiying Tian · Chenchen Qiu · Xiaohua Ma · Yanbao Fu**

Received: 6 July 2010 / Revised: 11 November 2010 / Accepted: 15 November 2010 / Published online: 1 December 2010


**Abstract** Assembly of Sn on Cu Nanorods as anode for Li-ion microbatteries was prepared by a two-step electrodeposition design. Firstly, Cu nanorods arrays were grown on copper substrate by anodic aluminum oxide template-assisted growth method. Then, Sn was deposited onto Cu nanorods arrays by galvanostatic deposition. X-ray diffraction and scanning electron microscopy measurements reveal that Cu nanorod arrays are covered with Sn. Electrochemical performances of prepared electrodes were evaluated by charge/discharge cycle measurement. The assembly of Sn on Cu nanorods electrode exhibited highly reversible specific capacity and superior capacity retention resulting from the three-dimensionally nano-architectured design, which exhibits a large surface area, shortened Li-ion diffusion distance, Cu–Sn alloying, and can accommodate the volume expansion of Sn during cycling. Deposition time is an important parameter for fabricating the assembly of Sn on Cu nanorods electrode with suitable structure and morphology.

**Keywords** Nanorods · Electrochemical properties · Electrodeposition · Alloys

## Introduction

There is great interest in developing rechargeable lithium ion batteries with high energy capacity and long cycle life for application in portable electronic devices, electric vehicles and implantable medical devices [1–6]. Tin is an attractive anode material for lithium ion batteries, due to its low discharge potential and high theoretical charge capacity (991 mAh $g^{-1}$) [7]. The Sn anode has a theoretical specific capacity nearly three times that of graphite anodes, but has found limited application because of its large volume change, reaching up to 360% in the alloying and dealloying processes of Li–Sn, which results in pulverization and capacity fading [4, 7–12].

At present, there are two methods to improve the cycling performance of Sn-based anode materials. One is adopting mixed-conductor matrix to form active/inactive alloy system. This method can partly relieve the large volume change and pulverization happening in the process of insertion and extraction of lithium for metallic anode materials [11–15]. The other method is using nanosized Sn based anode materials, which can also reduce volume change and restrain stress [16–18]. However, the effect of buffering of inactive phases matrix is limited, and nano-sized materials have a large surface area which easily cause particles aggregating [16].

The concept of using three-dimensional (3-D) nanostructured electrode has been demonstrated with $Fe_3O_4$ [2, 3], Si [1], Sn [8], $SnO_2$ [4, 19], $LiMn_2O_4$ [20], and $LiFePO_4$ [21], and has shown improvement in the rate capability and cycling performance compared to film and bulk materials. The 3-D nano-architectured electrode has several advantages [1–3, 13, 20, 22], such as the nano-architectured electrode allows for better accommodation of the large volume changes, the nano-architectured electrode allows for fast surface reaction resulting from large electrode/electrolyte interface area and the nano-architectured electrode has short Li-ion transport path compared with bulk material.

In this study, we prepared an assembly of Sn on Cu nanorods electrode, which is expected to accommodate large

D. Jiang · H. Tian · C. Qiu · X. Ma · Y. Fu (✉)
Department of Materials Science, Fudan University,
220 Handan Road,
Shanghai 200433, China
e-mail: yanbaofu@fudan.edu.cn

strain and shorten the lithium ion diffusion path. Our two-step electrode design consisted of the anodic aluminum oxide (AAO) template-assisted growth of Cu nanorods onto Cu substrates as current collectors and the electrochemical deposition of Sn onto Cu nanorods. The structure and electrochemical performance of the prepared electrodes were investigated.

## Experimental

### Fabrication of Cu nanorod arrays as current collectors

A thin film of Cu was prepared by sputtering Cu target onto one side of the AAO template (purchased from NANOPY; thickness 60 μm, diameter 12 mm) and severed as substrate. Next, the film was thickened by electrodeposition, which ensured the structural integrity of the nanostructured electrode after AAO template was removed. In the process of deposition, the other side of AAO template was protected from deposition by isolating adhesive film.

The Cu nanorod array on the Cu substrate was prepared via cathodic electrodeposition from an electrolytic bath consisting of $CuSO_4$ (225 g $l^{-1}$), $H_2SO_4$ (60 g $l^{-1}$) and NaCl (45 mg $l^{-1}$), inside the pores of the AAO template. The electrochemical depositions were carried out at a constant current of 30 mA $cm^{-2}$ at room temperature. The AAO templates served as the cathode, and a Pt sheet served as the anode. After the electrodeposition, the cathodes were immersed in a 2.0 mol $l^{-1}$ NaOH solution for 20 min to remove the AAO templates, and then cleaned in a dilute HCl solution to remove the surface oxides.

### Electrodeposition of Sn

Sn was deposited on the nanostructured Cu current collectors by electrodeposition. The electrolyte consisted of $SnSO_4$ (25 g $l^{-1}$), $H_2SO_4$ (40 g $l^{-1}$) and gelatin (20 g $l^{-1}$). The electrodeposition was carried out at a constant current density of 10 mA $cm^{-2}$. The Cu film sheet with Cu nanorods served as the cathode and a Pt sheet served as the anode. After electrodeposition, samples were rinsed with deionized water and dried in air. Sn was also electrodeposited on planar Cu substrates under the same condition for comparison with 3-D nano-architectured electrodes.

### Structure and morphology characterization

The structure and morphology of prepared assembly of Sn on Cu nanorods electrodes were characterized by X-ray diffraction (XRD, RIGAKU D/MAX-γB, $CuK_\alpha$) and field-emission scanning electron microscopy (FE-SEM, Philips XL30) equipped with energy dispersive X-ray spectroscopy (EDS).

### Electrochemical performance evaluation

The electrochemical performance of prepared electrodes was evaluated in coin-type half cells. Coin-type half cells were assembled using the assembly of Sn on Cu nanorods as the cathode and lithium metal as the anode. Cathode and anode were electronically separated by Celgard 2400 separator saturated with 1.0 mol $l^{-1}$ $LiPF_6$ electrolyte solution (in EC/EMC/DMC, 1:1:1 in mass ratio). The half cells were galvanostatically cycled between 0.001 and 2.0 V (vs. $Li/Li^+$) at 0.1 C rate (99.1 mA $g^{-1}$). The charge/discharge cycle and the capacity retention ability of nano-architectured Sn electrodes were studied.

## Results and discussion

### Morphology and structure characterization of assembly of Sn on Cu nanorods

Figure 1 shows the top and cross-sectional views of the Cu nanorod array prepared with 1 min electrodeposition. We can see that the Cu substrate is covered with uniformly

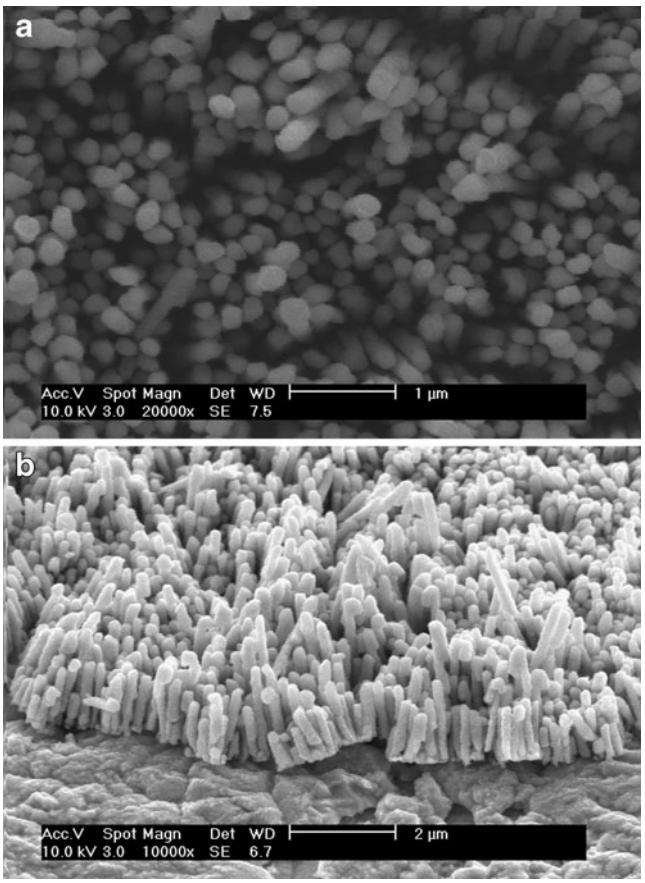


**Fig. 1** SEM images of Cu nanostructured current collector: **a** top view, **b** cross-sectional view

distributed and free standing Cu rods with average diameter of ca. 250 nm, defined by the pore size of the AAO template [2, 3], and a uniform height of about ca. 2.0 μm.

Figure 2 shows SEM images of as-prepared assembly of Sn on Cu nanorods and Sn deposited for 1 min. From the top view of the SEM image (Fig. 2a), we can observe that the morphology of assembly of Sn on Cu nanorods is similar to that of the previous Cu nanorods array. The oblique view (Fig. 2b) demonstrates that Sn was deposited on the surface of individual Cu nanorods. The corresponding EDS spectroscopy analysis, shown in Fig. 3, indicates that the surface of deposit on the copper nanorod contains Sn, which confirms the presence of Sn in the prepared sample.

Figure 4 shows the XRD pattern of as-prepared assembly of Sn on Cu nanorods electrode after Sn deposition for 1 min. The two strong peaks at around 43° and 51° correspond to the Cu (111) and Cu (200) reflections (JCPDS card no. 04-0836), respectively, originating from Cu substrate and Cu nanorods. The peaks at 30.5°, 31.9° and 44.8° are assigned to (200), (101) and (211) reflection of Sn phase (JCPDS card no. 89-2958), respectively. A $Cu_6Sn_5$ phase is observed in addition to Sn and Cu in the as-prepared sample. The weak peaks at 30.1°, 35.2°, 53.4° are assigned to the $Cu_6Sn_5$ phase [23]. This result indicates that the electrodeposition process formed a slight Sn–Cu intermetallic compound, which probably formed at the interface between tin and copper. The XRD pattern also confirmed the formation of Cu nanorods–Sn assemblies.

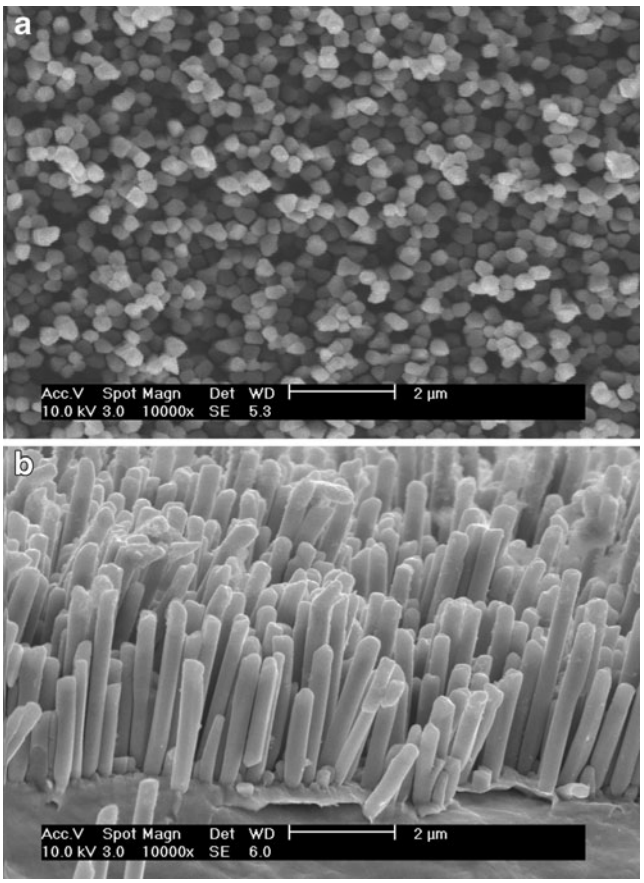


**Fig. 2** SEM images of as-prepared Assemblies of Sn on Cu nanorods (deposition time: 1 min): **a** top view, **b** oblique view

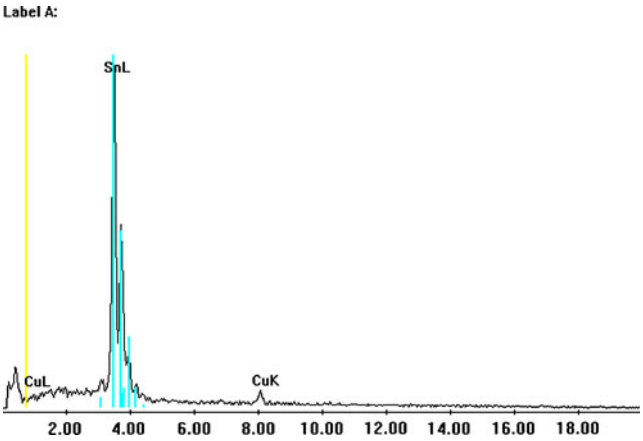


**Fig. 3** EDX spectrum of as-prepared assemblies of Sn on Cu nanorods (deposition time: 1 min)

Figure 2 shows that after Sn was deposited onto Cu nanorod, the Cu nanorod array maintained its original nano-architecture, which is crucial to gain the advantage of nanostructure such as large surface area, shortened Li-ion diffusion path and buffering space. But with Sn depositing time increasing (3 min), Sn on the tip of each Cu nanorod began to coalesce to form an un-compact film, as shown in Fig. 5a. Needless to say, the top of nanorod array would be covered with a continuous layer and the space among Cu nanorods would be filled with Sn with the deposition time increasing (Fig. 5b).

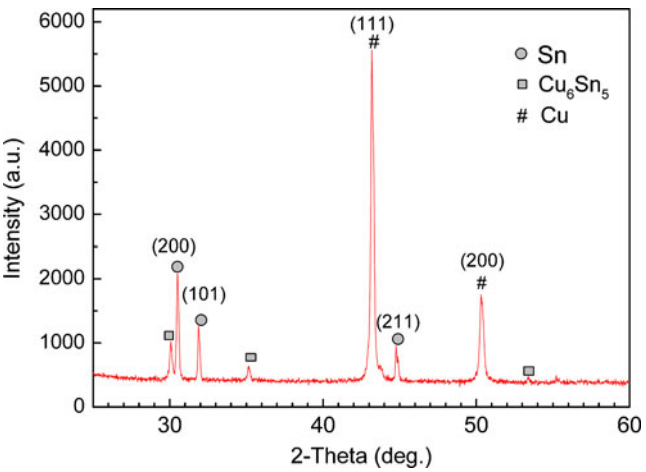


**Fig. 4** XRD pattern of assemblies of Sn on Cu nanorods (deposition time: 1 min)

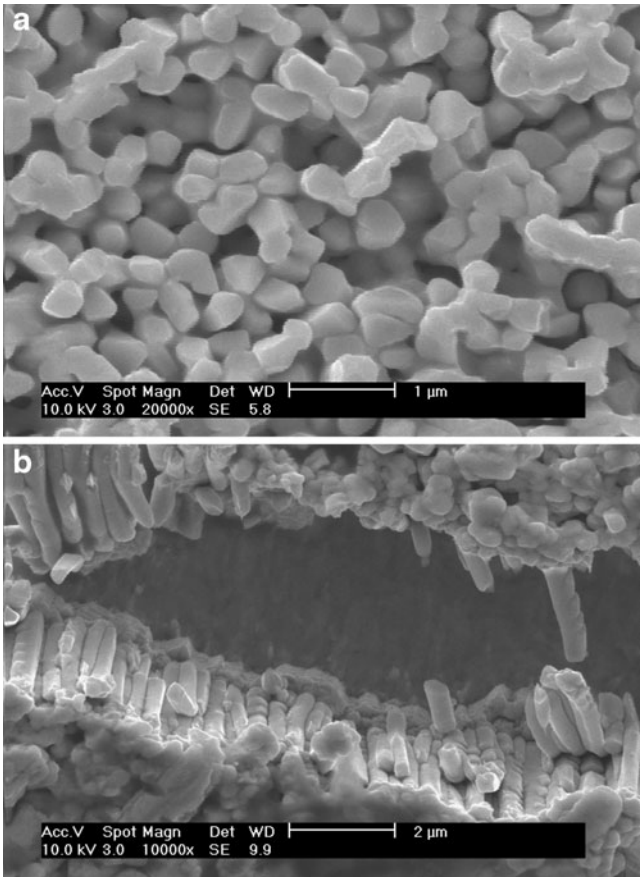


**Fig. 5** SEM images of as-prepared assemblies of Sn on Cu nanorods (deposition time: 3 min): **a** top view, **b** oblique view

## Electrochemical performance evaluation of assembly of Sn on Cu nanorods

It was reported that the assembly of Sn on Cu nanorods exhibits a higher capacity and better capacity retention than the other forms of Sn used in lithium ion batteries [8]. The electrochemical performance of our resulting assembly of Sn on Cu nanorods as electrode in lithium ion batteries were evaluated by charge–discharge cycles in a galvanostatic mode. Figure 6 shows the first and second charge–discharge cycles of test cells with assembly of Sn on Cu nanorods (Sn deposited for 1 min) as electrode at 0.1 C rate (99.1 mA $g^{-1}$). The voltage profile shows a long slope plateau below 1.0 V (vs. $Li/Li^+$) in the charge process corresponding to Sn reacting with Li to form the $Li_xSn$ alloy, but shows dealloying in the discharge process [10]. The plateau at 0.4 V during the charge stage is assigned to the formation of $Li_2CuSn$ from $Cu_6Sn_5$/Li alloys [24], which further confirms the existence of $Cu_6Sn_5$ alloy in the prepared assembly of Sn on Cu nanorods. The observed capacity during the first charge operation was 791 mA h $g^{-1}$, which is 80% of the theoretic capacity. The first discharge capacity was 727 mA h $g^{-1}$, indicating a coulombic

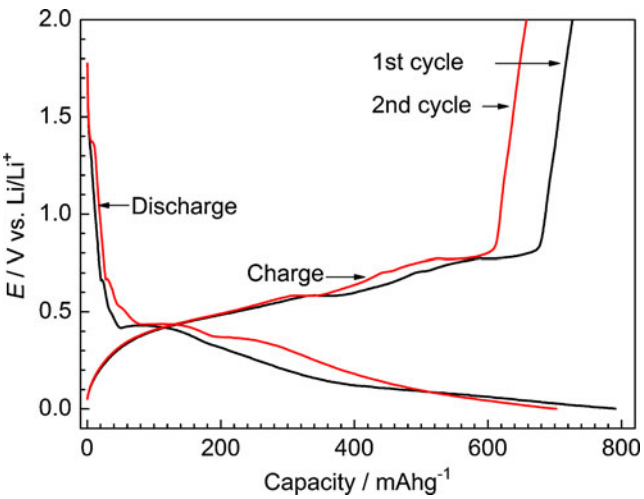


**Fig. 6** Voltage profiles for the first and second galvanostatic cycles of assembly of Sn on Cu nanorods electrode at 0.1 C rate

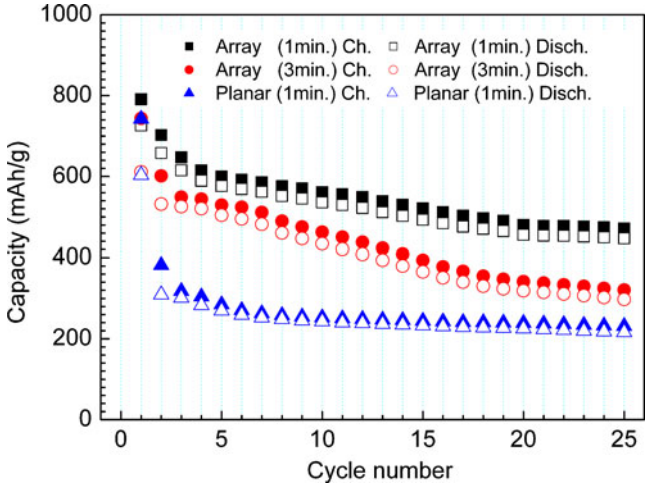


**Fig. 7** Capacity versus cycle number for assembly of Sn on Cu nanorods at the 0.1 C rate

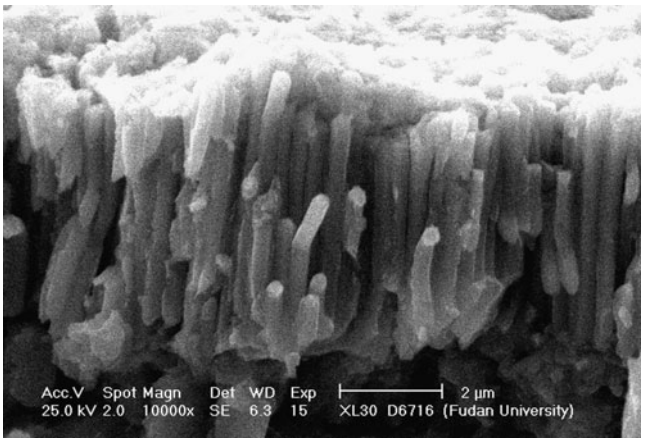


**Fig. 8** SEM image of assembly of Sn on Cu nanorods electrode (deposition time: 1 min) charged and discharged after 50 cycles

efficiency of 92%. The second charge capacity decreased by 11% to 702 mA h $g^{-1}$, and the second discharge capacity was 658 mA h $g^{-1}$, giving a coulombic efficiency of 94%. In the second charge process, we can observe an anomalous short plateau at about 1.4 V, which was previously reported by other research groups at about 1.6 V [1, 23]. It is generally attributed to the decomposition of the electrolyte during the early stage of lithiation catalyzed by very clean tin produced during de-lithiation. Both charge and discharge capacities decreased slowly in the subsequent cycles, and remained nearly constant after the 20th cycle (Fig. 7). The discharge capacity was 471 mA h $g^{-1}$ at the 25th cycle, remaining 60% of the first cycle.

For assembly of Sn on Cu nanorods electrode with 3 min deposition time, the capacity decreased rapidly along with the cycle number, compared to the sample deposited for 1 min. The capacity behaviors of the tested assembly of Sn on Cu nanorods electrodes are related with their structure and morphology. In the preceding section, we noted that Sn on the tip of each Cu nanorod began to coalesce to form an un-compact film and the space among nanorods was filled with Sn with deposition time increasing, which would block the electrolyte accessibility to the space among rods, and volume buffering of Sn could not be achieved during discharge and charge. This resulted in a poor capacity retention ability. Thus, deposition time is an important parameter for the assembly of Sn on Cu nanorods electrode.

As a comparison, in Fig. 7 charge and discharge data corresponding to assembly of Sn on Cu nanorods electrode are shown along with the charge capacity of a thin film planar Sn electrode which was fabricated by electrodeposition under the same conditions (10 mA $cm^{-2}$ of current density and 1 min for deposition). The planar electrode shows a dramatic decay in capacity with cycling due to the large volume change and pulverization, which is in agreement with the results reported by other groups [4, 7–12]. The improved capacity and cycle life for assembly of Sn on Cu nanorods electrode demonstrate the advantages of our 3-D electrode design. It can provide space buffering volume change of Sn during charge and discharge stages. At the same time, it can form a larger surface compared to a planar electrode with the same deposition time. In the previous section, the existence of Sn/Cu alloy phase was confirmed by XRD pattern and the alloy phase mainly formed at the interface between copper and tin. Hence, the large surface of the 3-D electrode can provide a larger surface to form the Sn/Cu alloy phase. Other researchers have reported that the Sn/Cu alloy electrode showed good retention ability and the existence of the alloy is helpful in keeping the electrode structure stable [23]. Thus, the formation Sn/Cu alloy phase also contributed to the improvement of the capacity retention of Sn on Cu nanorods electrode, which alleviates the pulverization of Sn and kept the electrode structure stable. This was confirmed from SEM observation of an electrode charged and discharged after 50 cycles, which revealed no peeling or other morphology changes, as shown in Fig. 8.

## Conclusions

Assembly of Sn on Cu nanorods electrodes for Li-ion battery was prepared via a two-step electrochemical process. The process consists of growing Cu nanorods onto a copper substrate by electrodeposition through AAO template and electrodeposition of Sn. The uniform and free-standing Cu nanorods with an average of diameter of 250 nm were deposited on the Cu substrate and the active material of Sn was grown on the surface of Cu nanorods. The assembly of Sn on Cu nanorods electrode exhibited highly reversible specific capacity and superior capacity retention. We achieved a charge capacity of 471 mA h $g^{-1}$ up to 25 cycles at the rate of 0.1 C. It was demonstrated that the superior electrochemical performance achieved using the three-dimensionally nano-architectured design, which exhibits a large surface area, shortened Li-ion diffusion distance and Sn/Cu alloy phase accommodating the volume expansion of Sn during cycling. Deposition time is an important parameter for fabricating assembly of Sn on Cu nanorod electrodes with suitable structure and morphology.

**Acknowledgement** This work was financially supported by Shanghai Leading Academic Discipline Project (Project Number: B113).

## References

1. Chan CK, Peng HL, Liu G, McIlwrath K, Zhang X, Huggins R, Cui Y (2008) High-performance lithium battery anodes using silicon nanowires. Nat Nanotechnol 3:31
2. Taberna PL, Mitra S, Poizot P, Simon P, Tarascon JM (2006) High rate capabilities $Fe_3O_4$-based Cu nano-architectured electrodes for lithium-ion battery applications. Nat Mater 5:567
3. Duan HN, Gnanaraj J, Chen XP, Li BQ, Liang JY (2008) Fabrication and characterization of $Fe_3O_4$-based Cu nanostructured electrode for Li-ion battery. J Power Sources 185:512
4. Li NC, Martin CR, Scrosati B (2001) Nanomaterial-based Li-ion battery electrodes. J Power Sources 97–98:240
5. Idota Y, Kubota T, Matsufuji A, Maekawa Y, Miyasaka T (1997) Tin-based amorphous oxide: a high-capacity lithium-ion-storage material. Science 276:1395
6. Poizot P, Laruelle S, Grugeon S, Dupont L, Tarascon JM (2000) Nano-sized transition-metal oxides as negative-electrode materials for lithium-ion batteries. Nature 407:496
7. Courtney IA, Dahn JR (1997) Electrochemical and in situ x-ray diffraction studies of the reaction of lithium with tin oxide composites. J Electrochem Soc 144:2045
8. Whitehead AH, Elliott JM, Owen JR (1999) Nanostructured tin for use as a negative electrode material in Li-ion batteries. J Power Sources 81–82:33
9. Tamura N, Ohshita R, Fujimoto M, Kamino M, Fujitani S (2003) Advanced structures in electrodeposited tin base negative electrodes for lithium secondary batteries. J Electrochem Soc 150:A679

10. Winter M, Besenhard JO (1999) Electrochemical lithiation of tin and tin-based intermetallics and composites. Electrochim Acta 45:31
11. Yang J, Wachtler M, Winter M, Besenhard JO (1999) Sub-microcrystalline Sn and Sn-SnSb powders as lithium storage materials for lithium-ion batteries. Electrochem Solid-State Lett 2:161
12. Lee SJ, Lee HY, Jeong SH, Baik HK, Lee SM (2002) Performance of tin-containing thin-film anodes for rechargeable thin-film batteries. J Power Sources 111:345
13. Ke FS, Huang L, Jiang HH, Wei HB, Yang FZ, Sun SG (2007) Fabrication and properties of three-dimensional macroporous Sn–Ni alloy electrodes of high preferential (1 1 0) orientation for lithium ion batteries. Electrochem Commun 9:228
14. Shin HC, Liu M (2005) Adv Funct Mater 15:582
15. Tamura N, Fujimoto M, Kamino, Fujitani S (2004) Mechanical stability of Sn–Co alloy anodes for lithium secondary batteries. Electrochim Acta 49:1949
16. Besenhard JO, Yang J, Winter M (1997) Will advanced lithium-alloy anodes have a chance in lithium-ion batteries? J Power Sources 68:87
17. Courtney IA, Dahn JR (1997) Key factors controlling the reversibility of the reaction of lithium with $SnO_2$ and $Sn_2BPO_6$ glass. J Electrochem Soc 144:2943
18. Pereira N, Klein LC, Amatucci GG (2004) Particle size and multiphase effects on cycling stability using tin-based materials. Solid State Ionics 167:29
19. Wang Y, Lee JY, Zeng HC (2005) Polycrystalline $SnO_2$ nanotubes prepared via infiltration casting of nanocrystallites and their electrochemical application. Chem Mater 17:3899
20. Nishizawa M, Mukai K, Kuwabata S, Martin CR, Yoneyama H (1997) Template synthesis of polypyrrole-coated spinel $LiMn_2O_4$ nanotubules and their properties as cathode active materials for lithium batteries. J Electrochem Soc 144:1923
21. Sides CR, Croce F, Young VY, Martin CR, Scrosati B (2005) A high-rate, nanocomposite $LiFePO_4$/carbon cathode. Electrochem Solid-State Lett 8:A484
22. Long JW, Dunn B, Rolison DR, White HS (2004) Three-dimensional battery architectures. Chem Rev 104:4463
23. Tamura N, Ohshita R, Fujimoto M, Fujitani S, Kamino M, Yonezu I (2002) Study on the anode behavior of Sn and Sn–Cu alloy thin-film electrodes. J Power Sources 107:48
24. Bazin L, Mitra S, Tarberna PL, Poizot P, Gressier M, Menu MJ, Barnabé A, Simon P, Tarascon JM (2009) High rate capability pure Sn-based nano-architectured electrode assembly for rechargeable lithium batteries. J Power Sources 188:578